JOURNAL OF APPLIED ELECTROCHEMISTRY **27** (1997) 839–845

On texture formation of nickel electrodeposits

C. BERGENSTOF NIELSEN, A. HORSEWELL

Materials Department, Risø National Laboratory , DK-4000 Roskilde, Denmark

M. J. L. ØSTERGÅRD

Institute of Process Technology, The Technical University of Denmark, DK-2800 Lyngby, Denmark

Received 22 April 1996; revised 10 October 1996

Electrodeposited nickel has been investigated by cross-sectional transmission electron microscopy and X-ray diffraction. The <1 0 0> fibre texture and fine-grained, dislocated columnar microstructure has been considered with respect to the mechanisms of growth during electrodeposition. Fine, codeposited nickel oxide hydroxide precipitates which have formed on the {1 1 1} planes appear not to have influenced texture formation. Although strong inhibition by adsorbed hydrogen or organic species is suggested from the work of others, this has not resulted in any codeposition of other species, either crystalline or amorphous.

1. Introduction

It is well known that the electrodeposition of nickel, in most cases, is associated with a certain fibre texture formation. By adjusting the plating parameters such as current density, pH value of the bath, additive type and concentration, and metal ion concentration, it is possible to obtain various textures. For deposits thicker than 100 nm the textures are completely independent of the crystal orientations of the substrate [1]. In additive-free Watts baths with pH values below 2.5, the textures that result are usually <1 1 0>, <1 0 0> or <2 1 0> depending on the overvoltage η [1]. Additives for the purpose of brightening the coatings can also alter the influence of pH and overvoltage on the texture.

Several hypotheses have been forwarded to explain the texture formation. Since electrodeposits usually exhibit very large residual tensile stresses, earlier theories [2–4] suggested that the texture is a result of a cold-work-like mechanism as seen in the plastic deformation which occurs during cold drawing of wires. A later hypothesis, which is also based on deformation due to deposition stresses, is that the texture is a result of a multiple twinning process [5].

Texture formation may alternatively be considered to arise from basic processes, that is, nucleation and growth of competing crystal surfaces, which may depend on the relative surface energies. Under some conditions kinetic effects during deposition may dominate.

At low current densities and high temperatures, the crystallites are oriented to the most densely populated atom plane parallel to the substrate. According to Finch's school [6–11] the deposited metal adopts the *lateral* type of growth. For f c c metals the axis of the preferred orientation is <1 1 1>, for b c c metals <1 1 0> and for h c p metals <0 0 0 1>. At low temperatures and high current densities the crystallites of the deposits are very often oriented so that the most densely populated atom row in the most densely populated atom plane is perpendicular to the substrate. Then the deposited metal adopts an *outward* type of growth; for f c c metals the axis of the preferred orientation is <1 1 0>, for b c c metals <1 1 1> and for h c p metals $<1\,1\,\bar{2}\,0>$ [12].

In many cases however there is strong preferred orientation in which the growth habit does not belong to either of these simple types. For the f c c metals the axes of orientation can be <1 0 0>, <1 1 2>, <1 1 3> and <2 1 0>. These orientations are now believed to arise from inhibition of certain three-dimensional growth facets.

Among others, Reddy [13] considers codeposited hydrogen at the cathode as an important parameter in inhibition during electrocrystallization. Reddy suggests that, depending on the plating conditions and hence the hydrogen adsorption on different $\{h\,k\,l\}$ crystal faces, the faces with the largest adsorption will have the slowest growth rate and it is therefore these faces that will develop. Amblard [1] also uses the concept of growth inhibiting species of other types. Not only does he consider codeposited hydrogen as an inhibiting species, but points also to organic compounds which are present as additives and to metal hydroxides which may develop as a result of local increases of pH in the Helmholtz double layer, which occurs at the electrolyte/deposit interface. Since the concentrations of the different growth-blocking species depend on plating conditions, it should be possible to control texture formation by controlling additives and plating parameters.

In this paper, we report on microstructural observations of cross-sections of electroplated coatings. These observations, together with selected area electron diffraction and X-ray diffraction are considered in the light of the above hypotheses.

0021-891X

2. Experimental details

The electrodeposit which has been investigated was obtained from a 'semibright' nickel bath. The bath contained 300 g dm^{-3} $NiSO_4 \cdot 6H_2O$, 40 g dm^{-3} H_3BO_3, 40 g dm^{-3} $NiCl_2$, 0.8 g dm^{-3} 37% formaldehyde and 0.4 g dm^{-3} Duplalux 538, which is a commercial brightener of the levelling type. The pH value was 3.6–4.4, the bath temperature 50 °C and the current density 200 A m^{-2}. A layer of approximately 150 μm of nickel was deposited onto a polycrystalline copper substrate. This type of plating bath is known to give semibright, columnar, <1 0 0> fibre-textured coatings, where the columns have a width of somewhere between 0.1 to 1 μm, at least when investigated using etching techniques and light microscopy or scanning electron microscopy (when the grains are examined using electron microscopy, they turn out to consist of even smaller grains). The <1 0 0> texture is known as the softest of the fibre-textured nickel coatings.

3. Observations

3.1. *X-ray experiments*

Using a conventional X-ray diffractometer operated in the 2-theta omega mode, it was found that the deposit exhibits a strong <1 0 0> texture; see the diffractogram in Fig. 1. The specimen was rotated about the normal to the coating during the measurement. The incident CuK_α radiation was from a copper X-ray tube operating at 40 kV and 30 mA. The total intensities of the peaks have been obtained by integration allowing for intensity factor correction. This gives a distribution of the lowest index reflections as follows; {1 1 1} < 4%, {2 0 0} = 91%, {2 2 0} < 1% and {3 1 1} < 5%.

As shown below, cross-sectional transmission electron microscopy investigations (XTEM) suggested the presence of nickel oxide hydroxide phases or other kinds of precipitates on {1 1 1} planes. Therefore the diffraction of such phases has been investigated. Because of the texture, this was done by tilting the sample by 54.7°, which matches the angular difference between {1 0 0} and {1 1 1} planes. Within a range of ± 3° the intensity of the {1 1 1} planes was found to be the same. Running this setup, a 2-theta-omega scan was made which would allow the suspected reflections to be revealed which were previously geometrically hidden because of the texture. The counting time and the collimation setup used gave a background intensity which was 60 times greater than the first diffraction experiment.

In Fig. 2 the 2-theta-omega scan is shown. The ordinate axis is chosen as logarithmic to enhance peaks of low intensity. Despite these efforts, no convincing additional peaks could be found at positions expected ($2\theta \approx 26°$–$28°$ for $d_{\text{precipitate}} \approx 0.32$–$0.34$ nm which is the calculated value from the electron microscopy diffraction results) for nickel hydroxide or related phases.

Long counting times were also used from $2\theta = 2°$ to 46° to investigate both the presence of codeposited amorphous and crystalline phases. The diffraction from an amorphous phase would present itself as a series of broad peaks at low angles (2θ between 2° and 20°) with falling maximum intensity for increasing θ. Again there is only a background signal in the diffractogram and it is concluded that there is below 1 volume per cent amorphous phase present.

3.2. *Cross-sectional transmission electron microscopy*

3.2.1. Sample preparation. For cross-section transmission electron microscopy (XTEM), a sample was cut and ground so that a cross-section of the substrate and the nickel deposit was less than 100 μm thick. The deposit was then electropolished in a perchloric acid–ethanol mixture using a modified window technique [14]. The penetration of the foil was about 50 μm from the substrate surface. Therefore

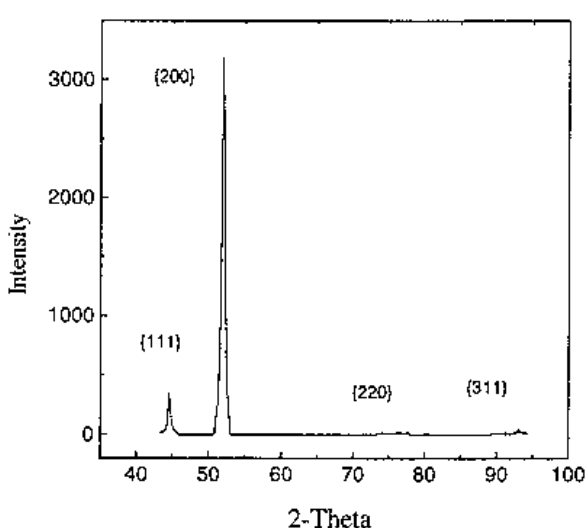

Fig. 1. 2θ-omega scan of the electrodeposited nickel sample, showing a strong [2 0 0] texture.

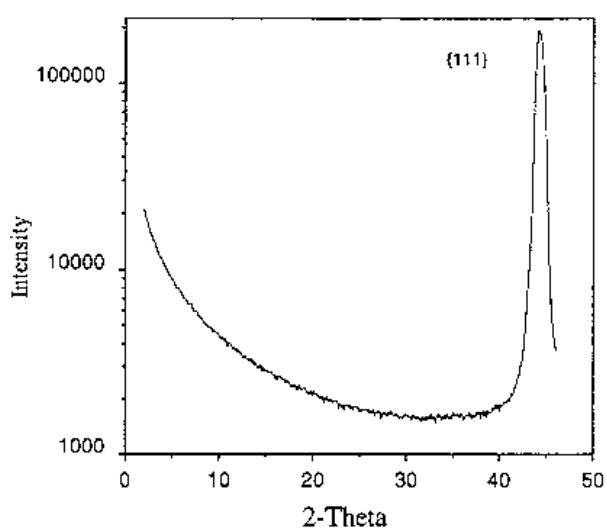

Fig. 2. 2θ-omega scan at low angles of the electrodeposited nickel sample.

the XTEM investigations presented below are only able to elucidate the part of the electrodeposit which corresponds to the stable growth condition. Neither the initial growth microstructure nor the transition zone of the deposit could be imaged successfully by XTEM.

3.2.2. XTEM investigation. The micrographs presented show the following features of the microstructure in the mentioned order. Columnar or fibre growth of grains, height and width of the fibres, microstructure of the grains which is highly dislocated/distorted, presence and orientation of precipitates in the fibre grains and twins in the thin regions of the sample.

Columnar growth: The columnar morphology of the nickel deposit is shown in Fig. 3. It is a dark field (DF) image showing many grown crystals with a large aspect ratio. They appear to have grown perpendicular to the substrate. The grain indicated by the pointer, is approximately 50 nm wide and 350 nm long, these being typical values for this microstructure. We denote these as fibre grains. The chosen reflection for the DF image in Fig. 3 is the {2 0 0}. The selected area diffraction pattern (SADP) of the area is seen in Fig. 4. The reflection that was used for the DF imaging is shown by the arrow. The angular spread of the reflections is about 20°, indicating a textured microstructure. On the DF image in Fig. 3 an arrow indicates the growth direction as well as the <2 0 0> direction of the nickel deposit. The <2 0 0> direction being approximately parallel to the growth direction is a general feature of the microstructure (see also the section on X-ray diffraction).

Distorted microstructure: At higher magnification (100 K) the fibre grains are seen to have a dislocated structure. In Fig. 5 a BF image of such fibres are shown. As it is a BF image, and as the crystals have the same <2 0 0> in common, it is hard to distinguish where the individual fibres begin and end. On the micrograph the direction of growth is indicated by the arrow. The micrograph is presented to give an idea of how much the microstructure is dislocated.

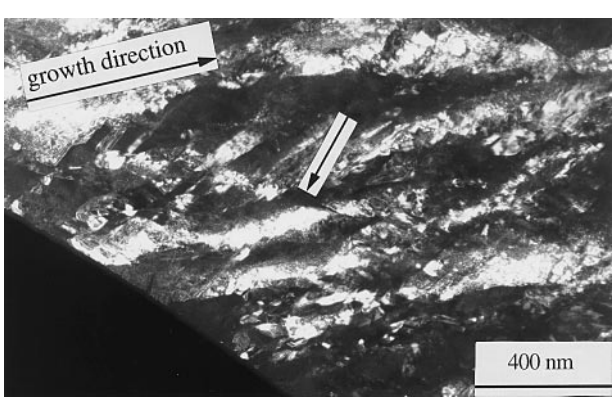

Fig. 3. Dark field image of columnar grains in the nickel deposit. A typical grain (50 nm × 350 nm) is indicated by the pointer. Diffraction spots used for imaging are indicated by the pointer in Fig.4.

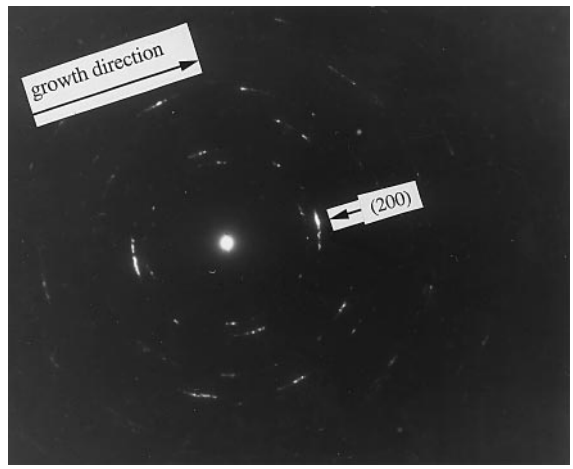

Fig. 4. SADP of the area seen in Fig. 3. The angular spread of the (2 0 0) spots is about 20°, indicating a strong texture.

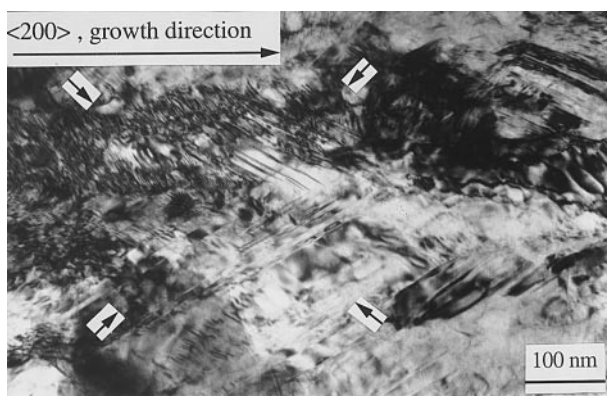

Fig. 5. Bright field image of a distorted columnar grain. Inside the square, made up by small pointers, there are features, probably microtwins, as they lie at about 55° to the <2 0 0> direction that corresponds to the habit planes.

An area on the BF image has been marked by a rectangle formed by four small pointers. Inside the rectangle a highly distorted microstructure is found. The features have an angle of approximately 55° to the <2 0 0> direction, that is, the growth direction, indicating that they are fine twins.

Precipitates: At magnifications greater than about 50 K, it is possible to find precipitates in the nickel grains. A DF image of such precipitates can be seen in Fig. 6. On the micrograph the arrow shows the <2 0 0> direction. The angle between the long side of the precipitate and the <2 0 0> is approximately 55° which is coincident with the angle of a {1 1 1} plane. Figure 7 shows the SADP from the microstructure in question. The pointer indicates which reflection was used for DF imaging. The reflection used for imaging the precipitate is parallel to the {1 1 1} reflection of the nickel, which suggests that there is an orientation relationship between the matrix and the precipitate. The precipitate reflection corresponds to a *d*-spacing of about 0.34 nm. The length of the largest precipitate area in the middle of the DF image is 170 nm and the height is 30 nm. The precipitate cluster consists of several individual crystals having a more or less plate-like geometry. The SADP in Fig. 7 shows streaking

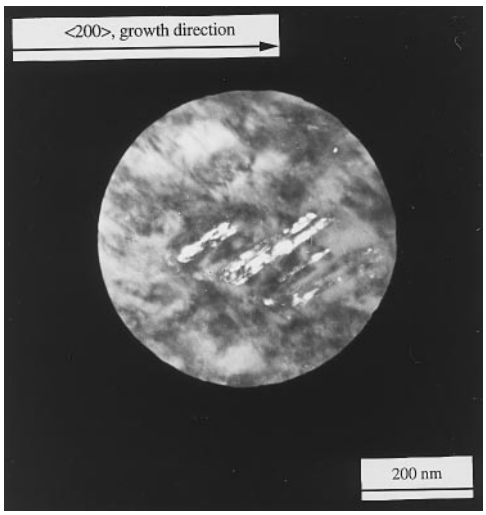

Fig. 6. Dark field image of precipitates lying on the habit planes of the nickel matrix. The length of the large agglomerate is approximately 170 nm, and the height is about 30 nm.

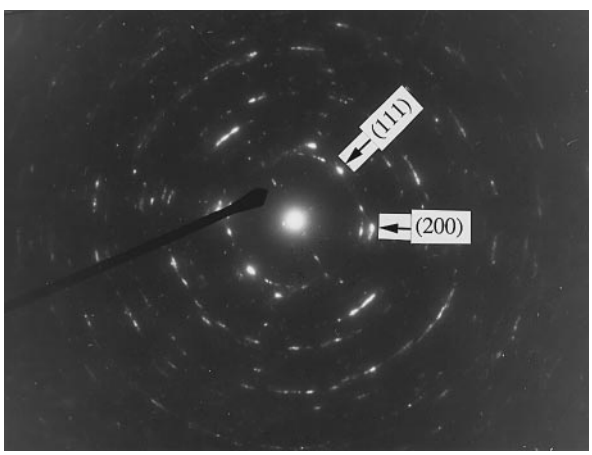

Fig. 7. SADP from the area seen in Fig. 6. The dark pointer indicates the reflection used for DF imagining. The reflection spot is parallel with the {111} reflection of the nickel matrix.

perpendicular to the thinnest dimension in the precipitates as expected due to the shape factor.

Using the powder diffraction files (PDF), the crystallography of nickel derivatives that could be expected to crystallize on the cathode during nickel electrodeposition (nickel oxides, hydroxides, oxide hydroxides, hydroxide hydrates, sulfate hydrates, sulfate hydroxides) have been investigated, and *d*-spacings have been compared with the measured value. Then γ-NiOOH (γ nickel oxide hydroxide is hexagonal with $a = 281.8$ pm and $c = 2056.9$ pm) fits the *d*-spacing criterion as the *d*-spacing $= 0.34$ nm fits the $d_{\{006\},\gamma\text{-NiOOH}} = 0.341$ nm within 10% deviation. The found precipitates have the same reflection parallel to the $<1\,1\,1>$direction of the nickel matrix, that is, there is an orientation relationship. It could therefore be suspected that the precipitates have deposited in an epitaxial manner. It has been tried to establish an epitaxial relationship between the (1 1 1) planes of the matrix and the (0 0 0 3) of the precipitate. Using stereographic projection it is found for the matrix that the angle between$(\bar{2}11)$ and $(\bar{1}2\bar{1})$ is 60°. Both the planes are perpendicular to the (1 1 1) plane. The lattice spacing is $d_{\{211\}} = 0.141$ nm. For the precipitate it has been found that the angle between $(2\,0\,\bar{2}\,0)$ and $(0\,2\,\bar{2}\,0)$ is 60°. The lattice spacing is $d_{\{200\}} = 0.143$ nm. Consequently, it is possible that the growth is epitaxial in the suggested way, as the angles are identical and the *d*–spacings within 1.4% also are identical. The shape and orientation of the precipitate shown in Fig. 6 is a general feature of the deposit although the volume fraction of the precipitates is low, estimated to be less than 5%.

Twins in thin areas of the sample: Figure 8 is a BF image, showing the edge of an electropolished hole in the sample: the rectangular area defined by the small arrows contain twins. Away from the edge the twins cease to exist. Figure 9 shows an enlarged part of Fig. 8. The twin planes indicated by the arrows are consistent with the {1 1 1} planes of the nickel. According to Gianuzzi *et al.* [15] the twins arise as an artifact of the preparation of the XTEM sample. High voltage XTEM on electrodeposited copper and palladium has shown that thin samples contain twins and have few defects, whereas the thicker samples contain more defects but no twins. Our observations

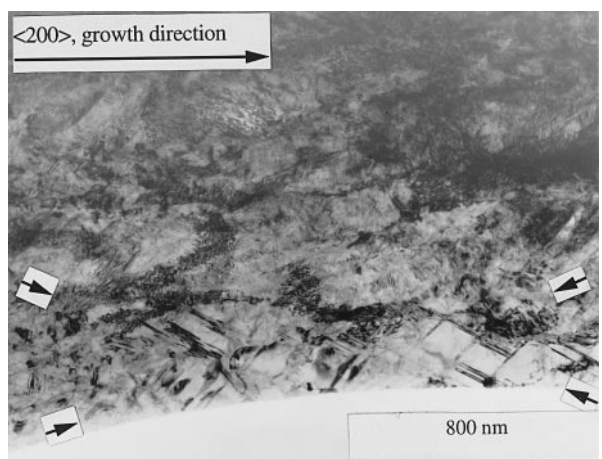

Fig. 8. Bright field image of the edge of an electropolished hole in the sample. There are twins at the outermost area of the wedge-shaped hole. As the sample becomes thicker away from the edge, the twins cease to exist.

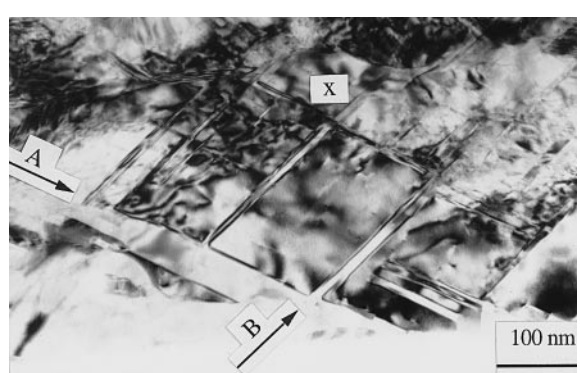

Fig. 9. Bright field image showing an enlarged part of Fig. 8. The image shows microtwins at the edge of the electropolished hole. The twin planes are indicated by pointers A and B. Note that cross twinning has occurred, for example, at point X.

are consistent with those of Gianuzzi *et al.* in which it appears that the twins form during TEM preparation to relax the elastic stresses imposed by dislocation loss due to image forces from the specimen surface. Accordingly, we also observe instances of cross-twinning.

Amorphous phase and cavities: Kinematical bright field images, under many-beam conditions have been used to determine if suspected amorphous phases and cavities could be imaged at grain boundaries. If an amorphous phase is present at grain boundaries, it will be seen as bright lines in under-focus conditions. It was not possible to obtain images which showed amorphous phases or cavities. Also, no evidence of an amorphous phase could be seen in the electron diffraction patterns. This evidence confirms the X-ray diffraction data.

Chemical composition: EDS analysis was conducted on the specimen. It was found that the chemical composition was 95% nickel and 5% cobalt. The $NiSO_4$ and the Ni anode used in the plating bath has been analysed using atom absorption equipment, and it was found that the anode and $NiSO_4$ contained about 2% Co. The Co content in the electrodeposited Ni is therefore believed to come from the anode and the $NiSO_4$. No precipitates of other chemical concentration values could be found, which suggests that the cobalt atoms are present as substitutional atoms.

4. Mechanisms of texture formation for electrodeposited metal layers

Growth leading to texture during electrodeposition has variously been considered to be a result of (i) a cold work mechanism, caused by large intrinsic deposition stresses; the texture formation is believed to result from the same plastic deformation mechanisms as that which occurs during cold drawing of wires, (ii) a multiple twinning process also caused by intrinsic stresses, (iii) the differences in the work of formation of different nuclei having crystallographic directions, (iv) an inherent difference in crystal face growth velocities due to differences in atomic density of crystal faces (the density of atoms can also be expressed as relative surface energy) and modification of these differences in growth velocity by hydrogen absorption and, (v) the presence of blocking or growth retarding agents, which inhibit the growth of certain crystal directions and allow other directions to grow.

Today there is in general very little belief in the hypothesis that preferred orientation of electrodeposits should stem from plastic deformation mechanisms or twinning mechanisms. This hypothesis has been rejected since Pd, Zn, Cd, Au and Ag can be electrodeposited with different preferred orientations of the crystals, and regardless of the texture axis, these electrodeposits have a very low residual stress. These earlier hypotheses will therefore not be reviewed. The interested reader can consult Wyllie [2], Bozorth [3], Wilman [4] and Rashkov *et al.* [5] for further information.

Pangarov [12] has carried out calculations on the work of formation of two dimensional crystals as a function of supersaturation. It is suggested that the texture results from a competitive nucleation of nuclei related to the work of formation. However, experimental data [16] shows that even under a strong epitaxial influence the same variety of three-dimensional nuclei are formed on to a nickel surface, whatever the current density and overvoltage. Further, calculations by Toschev [17] on three dimensional nuclei, have been carried out. The calculations suggest that the crystals will appear with different, but finite probabilities. This sequence is such that the probability of appearance of nuclei lying with a more densely packed face on the substrate is enhanced, that is, $P_{\text{nuc.}\{111\}} > P_{\text{nuc.}\{110\}} > P_{\text{nuc.}\{100\}}$ etc. [5]. Therefore, the hypothesis that texture results from a competitive nucleation, will neither be considered further.

More recent electrochemical studies of electrodeposition have suggested that the preferred crystal orientation in electrodeposits is a result of inhibition. Therefore the early and the extended inhibition hypothesis briefly will be reviewed before discussing the microstructural observations and diffraction experiments.

4.1. *Differences in growth velocity of crystal faces*

Texture development due to differences in the growth velocity of crystal faces is partly due to surface energy differences and partly due to kinetics of crystal growth. This hypothesis suggests that it is the difference in growth velocity of crystal planes of different indices $\{h\,k\,l\}$ that leads to faceting and hereafter texture of electrodeposited metals. Using a purely geometric argument, we see that fast growing faces grow out of existence, and slow growing crystal faces survive [18]. To understand the concept, consider a two-dimensional crystal with the shape of a rhombus, and let the upper line be a crystal face with a higher growth velocity to than the two lines with an angle to the upper line. As the lines grow outwards, the rhombus will get an upper line which becomes more and more narrow, and in the end the rhomboid shape has transformed into a triangle.

Then the densest faces will have the slowest growth velocity, v, meaning for the fcc case that $v_{\{111\}} < v_{\{100\}} < v_{\{110\}} < v_{\{211\}}$; this is the Bravais law of crystal growth. As an example, a growing fcc crystal with $\{1\,0\,0\}$ and $\{1\,1\,1\}$ faces would end up only leaving $\{1\,1\,1\}$ faces.

The Bravais law shows, however, only that crystal faces develop, but not in what way a given texture is produced. For the outward growth, Reddy [13] states: 'As the deposit crystals have an outward mode of growth, the velocity of growth in a direction parallel to the substrate surface is least.' The slowest growing facets should, therefore, be developed normal to the substrate. The axis of texture would then be the lattice row at the common intersection of the selectively developed facets (i.e., the zone axis). As an example,

the <1 0 0> texture of nickel should be a result of growth of {1 0 0} or {1 1 0} facets perpendicular to the substrate.

The above statements assume that the growing crystal faces do not experience any growth disturbing species. However, the electrochemical reactions that lead to the deposition of metal atoms, also involve generation of atomic and molecular hydrogen [1, 13, 19].

We may suppose that the presence of adsorbed hydrogen on the metal faces will slow down the growth velocity of a crystal face. The higher the indices of the $\{h\,k\,l\}$ face, the more chemically active the crystal face, the more adsorbed hydrogen, and therefore the more the growth velocity is slowed down. The presence of hydrogen therefore alters the mutual differences in growth velocities, and facets other than the {1 1 1} or the {1 0 0} can preferentially develop as they have a slower growth velocity than the lowest index facets. It must be expected that the concentration of the hydrogen, and the affinity to crystal faces of different $\{h\,k\,l\}$ is determined by pH value of the bath and overvoltage η. According to Reddy [13, 20, 21], these above arguments explain how changed bath conditions can change the texture of electrodeposits.

4.2. *Growth competition under influence of crystal face specific inhibitors*

Further considerations of crystal face specific growth inhibition is due to Amblard [1]. This can be divided into two major points or assumptions: (i) During electrodeposition, two- or three-dimensional nuclei are deposited, if not with the same probability in all directions, then with a finite probability distribution of the low index directions. (ii) During electrodeposition, different growth disturbing species are present on the crystal facets. These species may be hydrogen, hydrides, hydroxides or organic complexes depending on the bath chemistry and plating parameters.

4.2.1. Inhibiting species. Based on electrochemical impedance measurements, Amblard [1] shows that there are codeposited species that inhibit the deposition of nickel. A reasonable inhibiting specie is adsorbed hydrogen as it is generated as a part of the electrochemical process. Another inhibiting specie is believed to be $Ni(OH)_2$, which is caused by a pH rise in the electrolyte when H^+ ions arriving at a nickel cathode are discharged and adsorbed [22, 23]. Also, organic species may be adsorbed on the cathode and are added commercially to produce changes in morphology and alter the texture axes of electrodeposits [1, 24]

Assuming that there are inhibiting adsorbed species on the cathode, and that they are responsible for the texture formation, Amblard has performed several experiments that show what happens when more or less hydrogen is adsorbed on the cathode (for example through changed stirring conditions and pH value settings). Assuming that the concentration of hydrogen also controls the precipitation of $Ni(OH)_2$, this leads Amblard to conclude the following: The adsorbing species behave specifically on different crystal faces. When electrodeposits are textured, it is only one crystal direction which is not blocked in its growth, thereby creating a growth texture. It is the electrochemical conditions that decide the concentration of the individual adsorbed species and thereby the chosen texture.

5. Discussion

In the following we will discuss the texture formation theories reviewed above in the light of our own experimental results and the experimental results of others.

Our cross-sectional TEM (XTEM) results provide a quantitative impression of the growth processes during electrodeposition. The general morphology shows that the grains in the deposited film are columnar and highly textured. The grains are nevertheless small and dislocated and there are no clear facets. These microstructural features are inconsistent with a mode of growth strongly dominated by the development of low energy facets [13]. Such growth would produce a faceted final surface of the nickel deposit which is not observed. Also such a growth mechanism envisages facets which grow slowly perpendicular to the substrate. Then these facets, or remnants of facets, should be detectable in the electron microscope. In our case of a <1 0 0> texture there should be either {1 0 0} or {1 1 0} facets in the grown grains, which are not seen in XTEM. Some facet formation during electrodeposition does seem, however, to occur, as indicated by observation of small oxide hydroxide precipitates with {1 1 1} habit planes in the nickel matrix. Thus, at the time of co-deposition of precipitates, a well developed {1 1 1} facet was there to be deposited on. These precipitates are of approximately the same width, or less wide than the deposited nickel grains. In a comparable study Yan [25] shows using cross sectional electron microscopy, that during growth of zinc deposits there is a repeated codeposition of crystalline zinc oxides deposited as a result of varying chemical conditions in the cathodic double layer. Also, in the case of chromium deposition Snavely [19] has shown that chromium hydrides can be deposited.

The micrographs also show that the microstructure consists of outward growing crystals. According to Fischer [24], the field oriented fibre textured electrodeposits have their columnar growth as a result of inhibition of lateral grain growth. Inhibition may be caused by adsorbed hydrogen on certain crystal faces or by adsorption of organic species from the levelling additives. The extent to which inhibiting species such as hydrogen or organic species may or may not be codeposited depends on the stability of these species and the deposition kinetics, which again can be critically governed by the

plating parameters such as pH value, current density, concentration of additives, bath temperature and stirring conditions. However, some microstructural evidence of codeposition would be expected, either as included species or cavities from species lost after codeposition. Thus the absence of cavities could suggest efficient and continuous hydrogen desorption, or other inhibitor desorption.

The X-ray diffraction results showed that amorphous phases or organic species are not incorporated in the electrodeposited nickel. Also, no amorphous phase was seen at grain boundaries using TEM. There is therefore no indication that inhibiting species from the added brightener are sufficiently stable to be codeposited. Other evidence [1], however, shows that there is a clear inhibiting effect of organic additives on growth of certain crystal faces. Organic species, for example large aromatic molecules from added brighteners, will be incorporated in the microstructure [1]. The amount of incorporated organic species in the electrodeposit can be determined experimentally by measuring the concentration of brightener before and after deposition, see for example Amblard [1]. However, the aim of this investigation is not to determine this concentration, but to establish the presence of such in the microstructure or in other ways find evidence that there are or have been organic species in the microstructure. However, our X-ray diffraction and TEM results show that there is no significant presence of included amorphous co-deposits. Consequently, if the growth of electrodeposited nickel is affected by adsorbed inhibiting species, then the adsorbed specie must escape from the nickel before it is codeposited and incorporated. Kinetics may well be important in these processes and further studies are therefore required on the stability of codeposited nickel derivatives. Under some conditions, or in other systems, co-deposits may be more stable and therefore incorporated in the microstructure of the deposit.

6. Conclusion

The microstructure of a nickel electro-deposit has been investigated using cross sectional transmission electron microscopy and X-ray diffraction. It is found that the deposit has a <1 0 0> fibre texture and that there is a small volume fraction of precipitates on the {1 1 1} planes in the nickel. The precipitates are plate shaped and are less than 130 nm wide and less than 30 nm high. Diffraction evidence in TEM suggests that the precipitates are probably NiOOH. These small precipitates do not however appear to interfere with the nickel deposition. The nickel crystals grow in columns where the growth front is a pyramid, and where the faces of the pyramid are the {1 1 1} planes of the nickel crystal. Although there was an overall value of 5% cobalt in the nickel, the presence of precipitates with higher concentrations of cobalt could not be found.

Twins have been found in the microstructure, but only in the thin section of the TEM sample. Hence, these twins were not produced during electrodeposition. Instead they are deformation twins caused by the TEM sample preparation, which is also supported by the fact that cross-twinning has taken place.

The mechanism of texture formation in nickel has been suggested to arise through inhibition of growth of certain facets by the adsorption of hydrogen or amorphous organic species. Since there is an absence of amorphous phase and cavities in the microstructure of the nickel electrodeposit, such species are not incorporated in the deposit. Thus, inhibitors must apparently be sufficiently stable on certain crystal faces to modify growth while at the same time being sufficiently unstable so as to allow decomposition and/or release so as not to be codeposited.

Further systematic work on the microstructure dependency on plating parameters is required to understand the texture formation of electrodeposits. Especially for those metals in which preferred crystal orientation cannot be explained by lateral or outward growth controlled texture, such as is the case with nickel electrodeposits. It is suggested that the investigation should be performed with cross sectional electron microscopy of deposits produced over a range of deposition rates and bath chemistries in which inhibition effects are maximized. The effects that control the texture formation are probably the same that are known to cause trouble in the deposition in the outer regions of practicable electrodeposition parameters.

References

[1] J. Amblard, I. Epelboin, M. Froment and G. Maurin, *J. Appl. Electrochem.* **9** (1979) 233.
[2] M. Wyllie, *J. Chem. Phys.***16** (1948) 52.
[3] R. Bozorth, *Phys. Rev.* **26** (1925) 390.
[4] H. Wilman, Trans. *Inst. Metal. Finish.* **32** (1955) 281.
[5] S. Rashkov, D. Stoichev and I. Tomov, *Electrochim. Acta* **17** (1972) 1955.
[6] G. Finch, A. Quarrel and H. Wilman, *Trans. Faraday Soc.* **31** (1935) 1051.
[7] G. Finch and C. Sun, *ibid.* **32** (1936) 852.
[8] G. Finch and A. Williams, *ibid.* **33** (1937) 564.
[9] G. Finch and L. Yang, *Discussions Faraday Soc.* **1** (1947) 144.
[10] G. Finch, *Z. Elektrochem.* **54** (1950) 457.
[11] G. Finch and D. Layton, *J. Electrodepositors' Tech. Soc.* **27** (1951) 215.
[12] N. Pangarov, *J. Electroanal. Chem.* **9** (1965) 70.
[13] A. Reddy, *ibid.* **6** (1963) 141.
[14] J. Lindbo and T. Leffers, *Metallography* **5** (1972) 473.
[15] L. Giannuzi, P. Howell, H. Pickering and W. Bitler, *J. Elec. Mater.* **22** (1993) 639.
[16] J. Thevenin, *J. Microsc. Spectr. Electron.* **1** (1976) 7.
[17] S. Toschev, M. Pannov and R. Kaischew, *Izv. Otd. Khim. Nauki* **1**, (1968) 119.
[18] H. Buckley, 'Crystal Growth', J. Wiley & Sons, (1951).
[19] C. Snavely, *Trans. Electrochem. Soc.* **92** (1948) 537.
[20] A. Reddy and S. Ragagopalan, *J. Electronal. Chem.* **6** (1963) 153.
[21] *Idem, ibid.* **6** (1963) 159.
[22] A. Ives, J. Edington and G. Rothwell, *Electrochim. Acta* **15** (1970) 1797.
[23] S. I. Berezina, L. V. Burnasheva, A. N. Giĺmanov and R. M. Sageeva, *Elektrokhimiya* **10** (1974) 948.
[24] H. Fischer, *Electrodepos. Surf. Treat.* **1** (1972/73) 319.
[25] H. Yan, J. Downes, P. Boden and S. Harris, *Phil. Mag. A* **70** (1994) 391.